Admissible additional compressive stresses for ballastless track on railway viaducts: experiment and numeric analyses

Dipl.-Ing Marc Wenner *
M. Sc. Johannes Diers **
Univ. Prof. Dr.-Ing. Steffen Marx ***

* Marx Krontal GmbH, Beratende Ingenieure, Hannover, Germany, marc.wenner@marxkrontal.com
** Marx Krontal GmbH, Beratende Ingenieure, Hannover, Germany, johannes.diers@marxkrontal.com
*** Leibniz Universität Hannover, Insitute of Concrete Construction, Germany, marx@ifma.uni-hannover.de

Abstract:

Due to the track-bridge interaction and the constraining forces due to rail temperature, high compressive forces occur in the continuous welded rail (CWR) in the vicinity of bridge joints in the summer. By ballasted track, the high compressive stress state can lead to rail buckling. The stresses must be limited in order to avoid this fatal failure. In the case of ballastless track, the resistance of the track system is much higher than those of ballasted track. However, the values of the admissible additional compressive stresses given in the code for ballastless track are not based on any scientific background and are very conservative. In order to increase the admissible stresses in the rail compared to the actual code, additional fundamental investigations have to be performed. In this paper the theoretical investigation about the behaviour of one specific slab track system under high compressive forces will be shown. A large-scale experiment for a 31 m long track specimen has been designed and built to verify the theoretical results. This experiment will be presented, the measured results and their comparison with the results from the numeric model will be shown. To conclude, an outlook for the admissible compressive stresses for ballastless systems will be given.

Keywords: ballastless track; track bridge interaction; admissible stresses; buckling

1 Introduction and motivation

Regarding the design of long railway bridges, the track-bridge-interaction plays a decisive role [1]. Because of the connection of the rail with the superstructure, additional forces appear in the rail in the vicinity of bridge joints. In summer, the compressive forces due to track-bridge-interaction are superposed to the constraining forces due to rail temperature in the continuous welded rail (CWR) and leads to a high compressive stress state in the rail (Figure 1).

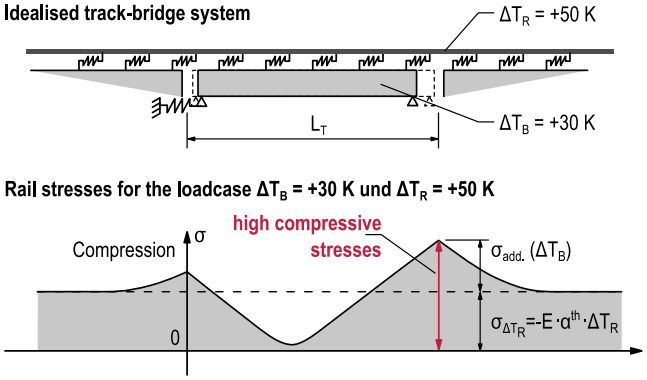

Figure 1: rail stresses due to the combined effect of temperature in the CWR and of track bridge interaction

Worldwide ballasted track is still used for the building of the conventional railway network. It is well known, that the limitation of compressive forces in the rail for ballasted track, especially on bridges, is necessary to avoid rail buckling. For the calculation of track-bridge interaction on long railway viaducts, a value of 72 MPa is given in DIN EN 1991-2 [3]. This value is based on extensive theoretical research work and experiments performed in Germany in the 1970s and 1980s. Further information concerning the background of this value can be found in [2].

In Japan, China as well as in Germany nowadays, ballastless track systems are used on High Speed Lines. For the calculation of additional rail stresses on bridges in this case, the value of 92 MPa accepted for tensile forces is transferred to the compression side, without any scientific background. But for the majority of ballastless track systems, engineers agree to the fact, that the resistance and rigidity of these systems is much higher than those of ballasted track. It can be expected that the ballastless system can carry much higher compressive rail forces than those allowed today.

In case of the Itz valley railway viaduct, an 868 m long viaduct on the new high-speed railway line between Ebensfeld (Bavaria) and Erfurt (Thuringia) the bridge was already finished at the time of the design and construction of the track. In the course of the detailed design of the ballastless track system, it was determined that the calculated additional rail

stresses exceed the admissible values of the code [4]. In order to tolerate the higher compressive stresses in the rail, fundamental investigations concerning the behaviour of the ballastless track system under high compressive forces have been performed. In this paper the large-scale experiment as well as the numeric investigations will be presented.

2 Investigated system and boundary conditions

The investigations have been performed on the ballastless track system ÖBB-PORR. The system consists of 5.16 m long elastically supported track base plates. The bottom of the plate and the openings are equipped with an elastic layer for decoupling. The track system on bridges is built on a concrete base layer connected to the bridge construction and fixed to it by grouting the tapered openings (Figure 2).

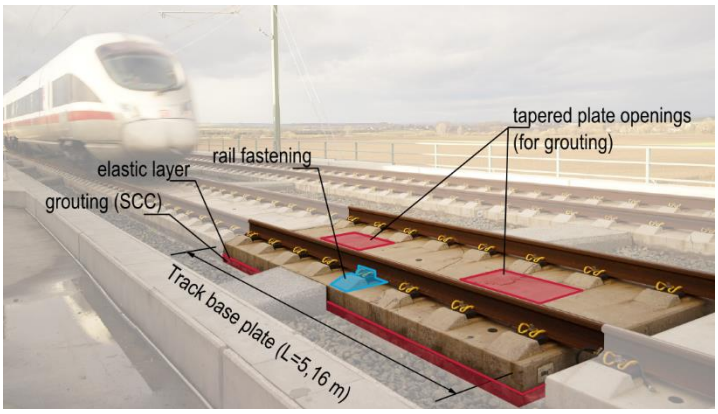

Figure 2: Ballastless track system ÖBB-PORR on bridges (Photo Marc Wenner)

Rail fastenings with reduced longitudinal restraint are used in the area of bridges (Figure 3a). Due to the additional forces in the fastenings in the area of bridge joints in case of lateral and vertical relative movements between neighboured superstructures, the 3 first fastenings on each side of the joint are special fastenings (Figure 3b).

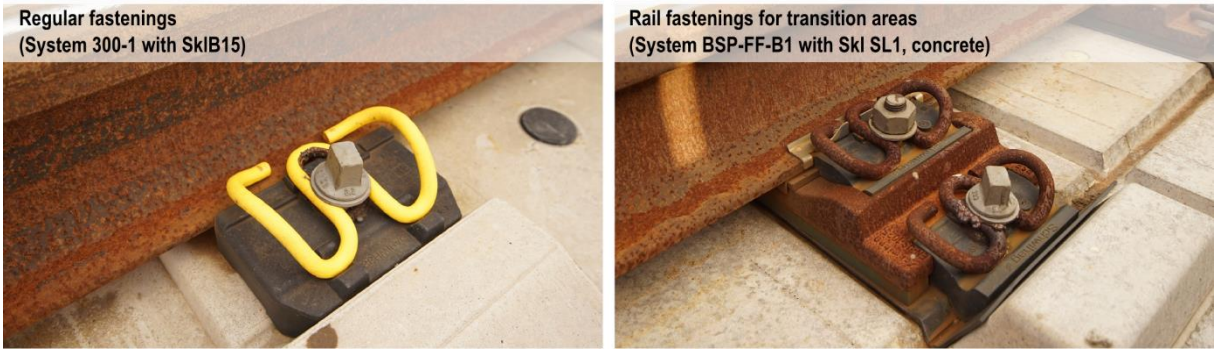

Figure 3: rail fastenings on ballastless track (a) regular fastening (b) fastening for transition area (Photos Marc Wenner)

For the determination of the admissible rail compressive stress the area of the bridge joint is decisive. As presented in Figure 1, the highest axial rail stresses occur in the area of the bridge joint. Furthermore, additional bending stresses occur in the rail in the vicinity of the bridge joint due to relative movement between neighboured superstructures. Because of the geometrical discontinuity over the bridge joint and because the special fastenings (Figure 3b) reacts less stiff than the standard ones, additional rail deformations occur. For the investigation of the behaviour of the rail under compression, the high stresses coupled with large imperfections are decisive. The experiments as well as the numeric analyses consider this area.

The rail stress level in the bridge joint area in case of CWR can be split in the following main parts:

- Constraining force due to temperature change of the CWR:
  climatic change: $T_{R,max}$ = +65°C
  possible additional warming due to eddy current brake: ΔT_R = +20K
  based on the minimal neutral temperature of the rail of 20°C in Germany, the maximum stress is:
  $\sigma_{TR} = -(85-20)\cdot 1{,}15\cdot 10^{-5}\cdot 210.000 = -157$ MPa.
- Effects of track-bridge interaction:
  in the actual code [3] the admissible additional compressive rail stress is $\sigma_{R,adm.add}$ = -92 MPa.

Expressed in a force, the actual axial stress level in the rail covered by the code is $F_R = -(157+92)\cdot 76{,}5\cdot 10^{-4\cdot} = -1{,}9$ MN (rail profile 60E2). The aim of the investigations presented in this paper is to increase this admissible force to show that the exceedance of the admissible values for the Itztal viaduct can be carried by the track system.

3 Approach

For the ballasted track large investigations have been performed in the 1980's in Germany. Since the behaviour of ballasted and of ballastless track differs from each other, the experiences and results cannot be simply transferred to the ballastless track system. A new approach for the investigations has to be defined. The different steps are:

1. Characterisation of the system, of its different components (e.g., material characteristics, stiffness) and of the parameters affecting the behaviour (e.g., imperfections, deformations)
2. Development of a first model, performing of numeric analyses to characterise the behaviour
3. Design and conducting of a small-scale and of a large-scale experiment
4. Comparison between numeric and test results, calibration of the model and update of the numeric analyses
5. Definition of limit states and limit values
6. Determination of the safety philosophy
7. Definition of admissible values for the compression stresses in the rail according a defined safety level

In this article, the steps 1 to 5 will be presented. Results of the steps 6 and 7 will be published later. The numeric analyses, the characterisation of the system as well as the information and results about the large-scale experiment will be presented in the following chapters.

Since the impacts of the system reactions are multiple and complex, limit states and limit values must be defined in order to identify critical parameters and to evaluate the admissible stresses. Therefore, different evaluation criteria have been classified in 3 limit states following the approach in the Eurocode EN 1990 [5]:

- **Ultimate limit state for material**
  criteria: stability failure (buckling of the system), failure of single components (rail, rail fastening, concrete of the track base plate)
  aim: ensure the integrity of the system
- **Ultimate limit state for rolling stock**
  criteria: track and rail geometry (longitudinal level, cross level, alignment and gauge)
  aim: ensure the riding safety of rolling stock
- **Serviceability limit state**
  criteria: excessive plastic deformations of the rail
  aim: ensure the serviceability of the system

If enough information is available in the codes, the related limit values are defined based on them. This concerns e.g. the failure strength of steel and concrete as well as certain track geometry limits. For the failure strength of fastenings, test results have been taken into account. For the definition of limit values of the alignment, additional simulations had to be performed (MBS multibody simulation).

In the entire process, the determination of the system characteristics and the definition of its resistance is very difficult. Because the system consists of many different components, a lot of very specific information is needed. Because the information is not available in codes or product information, additional investigations are necessary.

4 Large-scale experiment

Because of the geometric and material non-linearities of the investigated system, the behaviour is complex to describe. No experiences exist with the system under the considered situation. In order to ensure that the numeric results correlate with the reality, the execution and analyse of full-scale experiments were a central part of the investigations. In this paper the large-scale experiment will be presented.

For the design of the experiment, first numeric analyses according the described model in chapter 5 have been performed. Thereby the critical imperfections to consider as well as the interesting measurement areas could be determined. The aim of the large-scale experiment is to examine the behaviour of the complete system under realistic conditions. Therefore a 31 m long specimen of the ballastless track system ÖBB-PORR according the layout used on the bridge have been built on a test platform (figure 4). According to the preliminary numeric analyses the alignment corresponds to a curve with R=2200 m and short track base plates with only one opening have been chosen in order to lower the resistance of the system as much as possible. The critical bridge joint area as presented in chapter 2 has been reproduced in the middle of the specimen and represent the decisive investigation area (figure 4).

The maximum axial rail force for the design of the experiment is 4 MN in each rail. These forces were planned to be introduced with hydraulic jacks on one end of the rail. In order to introduce these forces into the system, a closed load frame has been built around the specimen (figure 4).

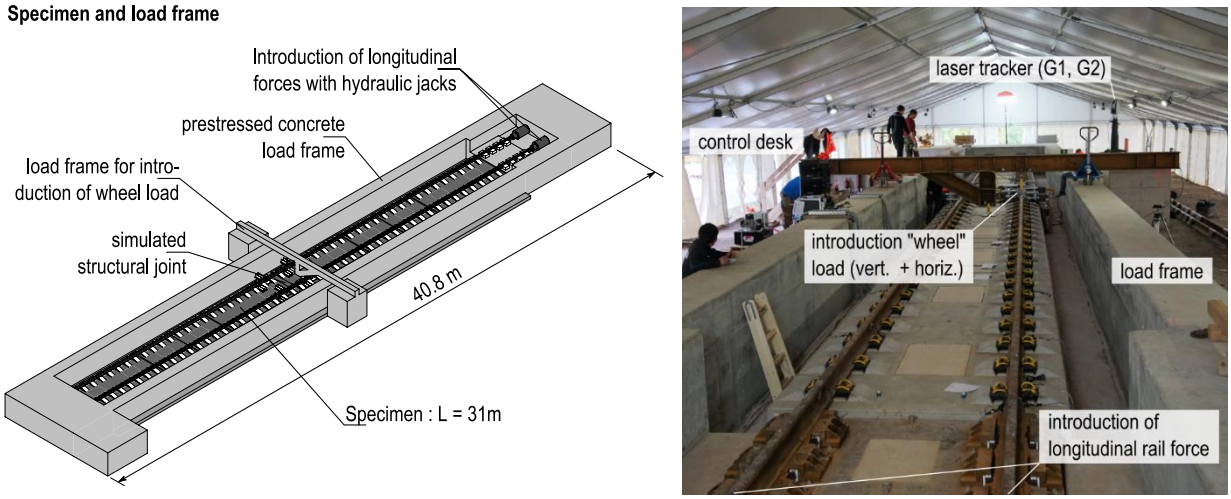

Figure 4: isometric drawing of the experiment and photo of the finished specimen

In addition to the longitudinal force in the rail, transverse forces had to be introduced in the rail to achieve the intended pre-deformation of the rail (figure 5) and to simulate the effect of wheel loads on the rail (figure 4).

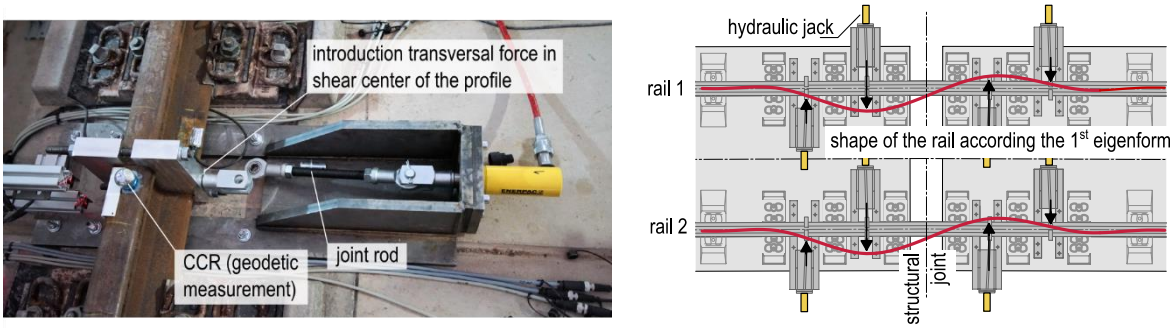

Figure 5: hydraulic jacks connected to the rail to introduce the intended pre-deformation of the rail: photo and deformation principle

In order to record the real geometry and to monitor the behaviour of the system while increasing the load in the rail, a specific measurement concept has been developed (selection of the major measurements):

- **Measurement G1**: Geodetic measurement of the initial position and shape of the fastenings and rails
  Therefore a laser tracker (Leica AT960LR) and a T-Probe enabled to record the absolute position of the measured points with an error <0,1 mm. By measuring the rail profile every 20 cm in the area of the joint a precise shape of the rail could be determined (G1 and G2 measured by the Geodetic Institute of the Leibniz University Hannover).
- **Measurement G2**: Geodetic monitoring of the absolute deformation of selected points
  By using the laser tracker and 66 Corner Cube Reflectors (CCR), the absolute displacement of the selected points while increasing the force could be recorded (including 12 CCR on each rail, 32 on the track base plate).
- **Measurement F**: Measurement of the introduced force in the rail
  By using 2 load cells, the force could be monitored to control the test.
- **Measurement S1**: Measurement of the longitudinal rails strains over the rail length
  because of the longitudinal rail restraint of the fastenings, the force decreases between the jacks and the investigated area in the centre of the specimen. Therefore, the force gradient has been recorded along the rail with strain gages.
- **Measurement S2**: Measurement of the rail strains on the edge of the rail foot
  In order to get information on the rail curvature due to bending, additional strain gages have been installed on the rail foot in the areas with high bending stresses (details in figure 6).
- **Measurement W**: Measurement of the relative transversal displacement of the rail
  One central criteria in the investigations concerns the rail displacement in the transverse direction. The relative displacements between rail and track base plate as well as the local rotation of the rail profile have been monitored by 2 laser displacement sensors (details in figure 6).

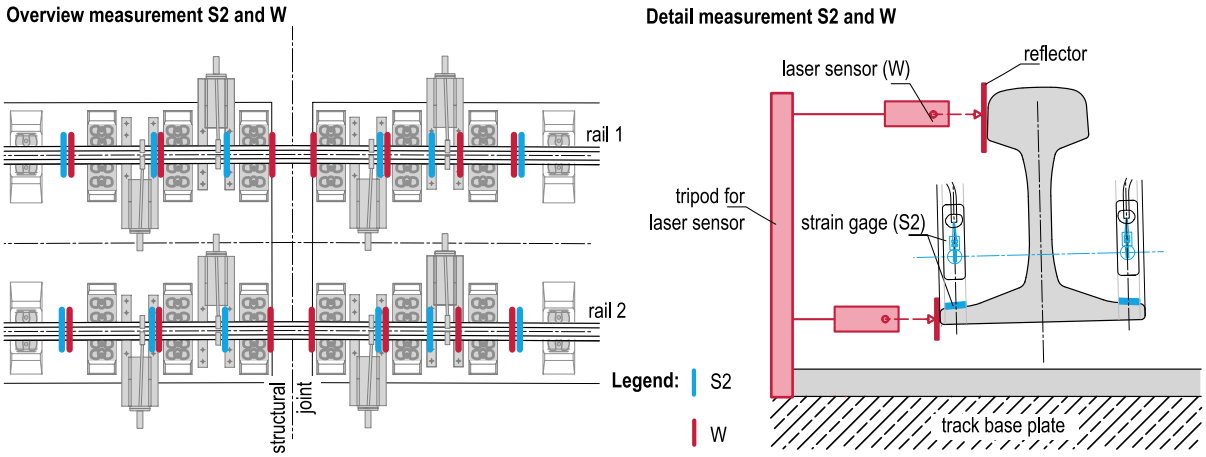

Figure 6: Details of the measurements S2 and W

The experiment has been performed twice to check if the behaviour is reproducible (total of 4 rails). Each of the 2 experiments consisted of several parts. In the first part the initial pre-deformation has been introduced in the rail by plastic deformations of the steel under the combined action of longitudinal and bending stresses. In the second part the force was increased up to the characteristic force to verify (2.1 MN). In the third and fourth part 1 resp. 2 fastenings have been demounted to simulate failed components. In the last part the force has been increased to the maximum. Between the different parts the rail has been decoupled from the fastenings to ensure that no initial lateral forces remain in the fastenings. In each part, the force has been increased step by step (steps of 500 kN). Each force has been repeated 3 times, in the 2nd and 3rd time the effect of the wheel load has been simulated.

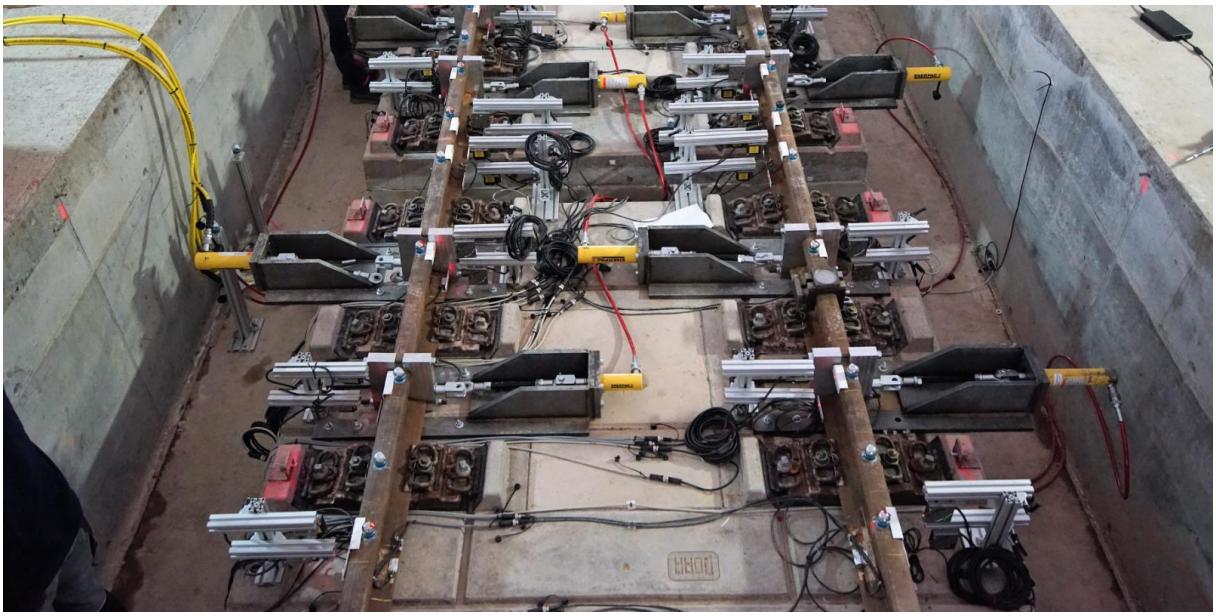

Figure 7: Photo of the investigated area in the centre of the specimen (structural joint)

5 Numeric analyses and results of the experiment

The numeric finite element model for the ballastless track follows the geometry of the specimen of the experiment. To reduce computation time, it however only consists of one rail (half-system, see Figure 8). The rail is represented by beam elements with the corresponding cross section and material model. In regular intervals these elements are supported by several springs with the stiffness properties of the support points and the slab itself. The model was built with the FE-software SOFiSTiK.

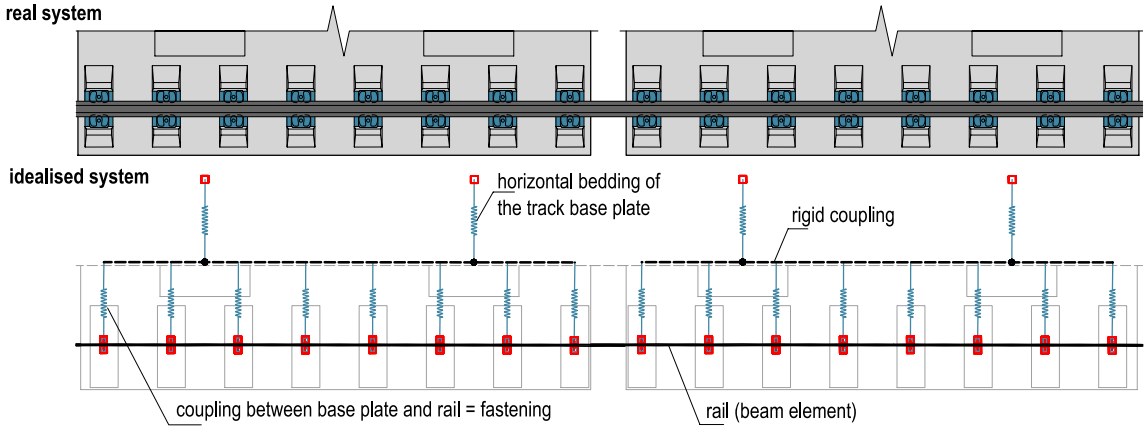

Figure 8: Schematic for the numerical model of the ballastless track half-system (top view)

In addition to the calculation methods of second order, the system contains nonlinear material properties for the fastenings and the rail (Figure 9). Although the rail is held down by tension clamps (Figure 3) it can move relatively easily in the lateral direction within a certain tolerance inside the supporting point. Once the rail foot makes contact with the guide plates the stiffness increases. This behaviour is even more pronounced for the special support points near the joint (Figure 3). The stress-strain-relationship of the rail steel has no pronounced yield point so the stiffness decreases continuously instead. The corresponding loss in bending stiffness of the rail itself has a big impact on the system reactions under high compressive loads. Therefore, an excessive conservative simplification of the material is not practical. The deformations of the track base plate itself were neglected, so that only a rigid-body motion of a whole slab is possible (rigid coupling between the nodes of the horizontal springs in Figure 8). This hypothesis could be verified in the test.

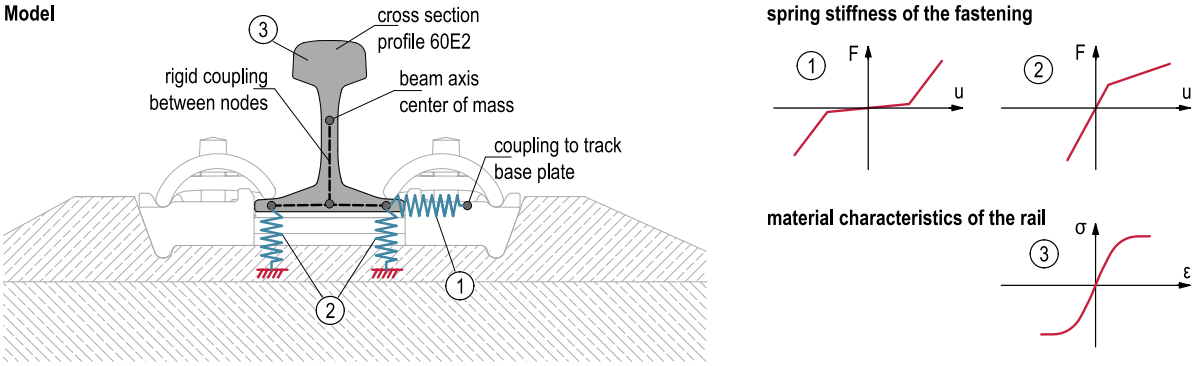

Figure 9: Numerical model of the rail and support points with material nonlinearities

For the numerical calculation the compression load of the rail is applied incrementally to analyse the changes in the system behaviour. To trigger the second order bending of the rail, lateral pre-deformations must be applied. These can consist of natural imperfections due to the manufacturing process of the rail and deformations from the bridge structures on which the track system is permanently connected (figure 10). The two separate superstructures of the bridge underneath can impose a relative lateral displacement and a relative rotation between the neighboured base plates at the joint. In reality it is most likely a combination of these influences that can trigger a nonlinear behaviour of the rail under high compressive loads.

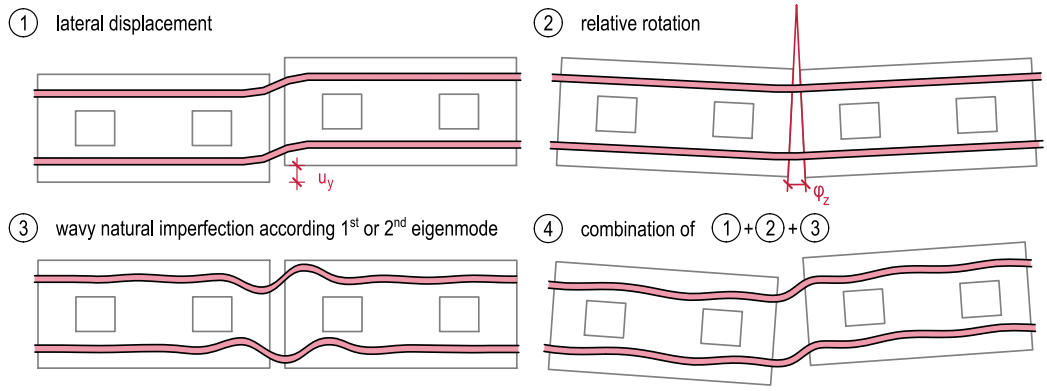

Figure 10: Possible pre-deformations of the system at a bridge joint

As expected the deformations of the rail stay relatively small until higher compressive loads are reached (figure 11). Only near the point of stability failure larger deflections occur. However, the development of the deformations depends on the used shape and magnitude for the pre-deformation.

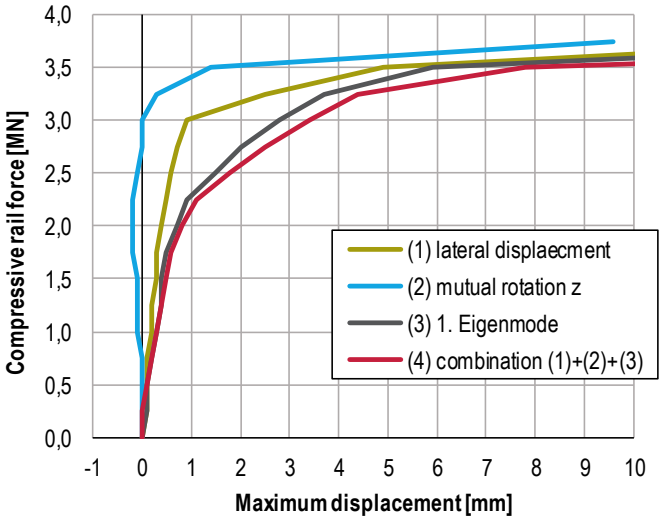

Figure 11: Force-deflection-diagram for different pre-deformations

In order to compare the numeric with the measured behaviour and to validate the numerical finite element model, the measured geometry of the rails from the experiment (measurement G1) was used to create a corresponding pre-deformation shapes for the model. The calculated results were then compared to the measured reactions of the tested rails. During the evaluation of the test results it became clear, that for the first part of the experiment the nonlinearity of the rail steel had an important impact on the system behaviour. In the later parts when the rail had already been loaded repeatedly the steel reacted more linearly and the deformations were smaller, which can be attributed to the hardening of the steel. This means that for the comparative calculations of each part of the experiment a correct approach for the material behaviour had to be chosen. It also means that for the further calculations to enable the determination of an admissible value of compressive stress, the nonlinear behaviour has to be assumed in order to be on the safe side.

In figure 12 the development of the deformed shape of the rail for a section in the area of the structural joint with increasing compressive force (figure 12a) is shown with the corresponding force-deflection-curves for the two points with the biggest displacements (figure 12b). Overall the comparison between the finite element model and the experiment led to a good match with the model tending to be on the safe side.

Other conclusions were that the vertical deformations of the rail as well as the movement of the base plates are negligibly small, as it was expected. Furthermore, in the experiment a maximum compressive load of 3.8 MN per rail was reached, which was much higher than the force to be verified in the case of the Itz valley bridge. For this stress level, high displacements of the rail were reached, but without any kind of stability failure or critical damage of system components. Beside the calibration of the model, the experiment showed also the high resistance and robustness of the system.

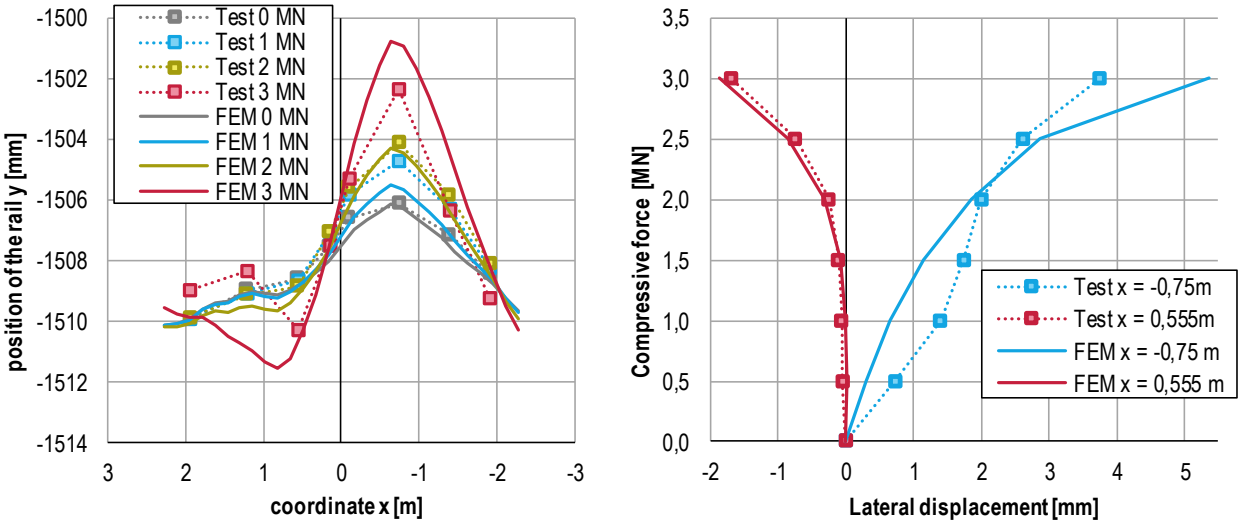

Figure 12: (a) Deformation shape of the rail and (b) force-deflection-diagram, comparison between experiment (Test) and finite element model (FEM)

6 Conclusion and Outlook

By checking the effects of track bridge interaction, the additional rail stresses have to be compared with admissible stresses given in the codes. For ballastless track systems, the actual limit value for compression is very conservative. The actual limit corresponds to a rail force of 1,9 MN. In order to increase the admissible stresses, specific investigations have been done.

The major conclusions from the performed experiments and numeric analyses are:

- The forces and displacements in the transverse horizontal direction are decisive
- The deformations of the rail are small (less than 4 mm by 3 MN in the experiment)
- A buckling of the system occurs by high forces: 3.75 MN in the numeric analyses, in the experiment no stability failure by the maximum force of 3.8 MN
- The serviceability criteria (yield stress of the rail steel) and the deformation of the rail and its impact on the riding safety of rolling stock are decisive. In the numeric analyses the criteria were met by 2.7 resp. 3.0 MN
- Even with 2 failed fastenings in the critic area of the joint, the stability limit is marginal smaller than for the intact system. The failure of fastenings impact however the ultimate limit state for rolling stock because of the higher rail displacements. Since the forces in the fastenings are much lower than their resistance, a fastening failure is improbable but has to be taken into account by deriving an admissible stress value for compression.

The maximum forces identified to meet the defined criteria cannot be directly translated in an admissible value to include in the verification of the additional rail stresses on bridge. The analyses have been performed for average values of parameters and resistances. In order to evaluate the admissible stresses, additional investigations including the consideration of the safety philosophy of actual codes [6], [7], sensitivity analyses and stochastic evaluations of the impacting parameters and resistance criteria have to be performed. These investigations are being performed currently.

The investigations performed in the last year give us important experiences about the behaviour of ballastless track when exposed to high axial compression rail stresses and enable the update of the actual codes. An increasing of the admissible additional compressive rail stresses can lead in the future to more freedom in the design of railway bridge and enable the avoidance of rail expansion joints in more situations than today.

At the Leibniz University Hannover further research work is being performed also concerning the admissible rail tension stresses. The results will be published soon.

7 References

[1] Wenner, M.; Lippert, P.; Plica, S.; Marx, S. (2016): Längskraftabtragung auf Eisenbahnbrücken, Teil 1: Geschichtliche Entwicklung und Modellbildung, in: Bautechnik 93, Heft 2, S. 59 – 67, DOI: 10.1002/bate.201500107

[2] Wenner, M.; Lippert, P.; Plica, S.; Marx, S. (2016): Längskraftabtragung auf Eisenbahnbrücken, Teil 2: Hintergründe des Nachweises, in: Bautechnik 93, Heft 7, S. 470 – 481, DOI: 10.1002/bate.201600034

[3] DIN EN 1991-2:2010-12: Einwirkungen auf Tragwerke –Teil 2: Verkehrslasten auf Brücken. DIN, Beuth Verlag.

[4] Wenner, M.; Wedel, F.; Meier, T.; Marx, S. (2018) Load testing on a high railway bridge to determine the longitudinal stiffness of the substructure, in Proceedings of the Sixth International Symposium on Life-Cycle Civil Engineering (IALCCE 2018), CRC Press, Taylor & Francis Group

[5] DIN EN 1990:2010-12: Grundlagen der Tragwerksplanung. DIN, Beuth Verlag.

[6] Eisenmann, J. (2002): Gleisstabilität von HGV-Strecken unter Berücksichtigung der linearen Wirbelstrombremse, in: EI- Eisenbahningenieur 53, Heft 5, S. 12 – 18.

[7] Freystein, H. (2012): Untersuchungen zu den zulässigen zusätzlichen Schienen-spannungen aus Interaktion Gleis/Brücke. Dissertation, Heftreihe des Instituts für Bauingenieurwesen der Technischen Universität Berlin, 2012.